Cause analysis and simulation verification of a 220kV GIS basin insulator along surface discharge

Xin Li[1,*], *Peilong* Chen[1], *Huarong* Zeng[1], *Xianyin* Mao[1], and *Kai* Liu [2]

[1]Electric Power Research Institute of Guizhou Power Grid Grid Co., Ltd., Guiyang, Guizhou 213022, China;
[2]Electric Power Research Institute of Southern Power Grid Company Limited Co., Ltd., Guangzhou 510000 Guangdong, China

Abstract. A surface discharge fault of 220kV GIS basin insulator during power transmission has been analyzed. Combined with on-site disassembly inspection, data from previous tests and structural design, the fault point is determined and the fault cause is preliminarily analyzed. In order to verify the correctness of the analysis results, this paper uses the finite element method to mathematically model the accident basin insulator, and formulates the boundary conditions for the calculation of the electric field inside the basin insulator. The simulation results show that there is a distorted electric field on the surface of the basin insulator, which is the main reason for creeping discharge. The preventive measures are summarized for the creeping discharge fault of the basin-type insulator to avoid the occurrence of similar accidents.

1 Introduction

Gas-insulated metal-enclosed switchgear, reabbreviated as GIS, is a fully enclosed combined electrical appliance, which encapsulates equipment such as busbars, circuit breakers, isolation/grounding switches, transformers, and arresters in a grounded metal shell to form a whole device [1-2]. Because of its reliability, safety, and small footprint, it has been widely used in power systems [3-4].

As the core component of GIS, basin-type insulators have a direct impact on the stable operation of the entire equipment and substations. The surface discharge of basin-type insulators is also a high-frequency fault of combined electrical appliances[5]. Therefore, it is of far-reaching significance to study the problems of basin-type insulator flashover, internal electric field distortion of GIS, and partial discharge[6-7]. Literature [8] conducted an electric field simulation analysis on the partial discharge or flashover caused by bubbles inside the basin insulator. Literature [9] summarizes the preventive measures during the transportation and installation of GIS in view of the insulation failure occurred in the AC withstand voltage test of GIS. Although the above-mentioned documents have a certain

* Corresponding author: 389768046@qq.com

degree of reference, they do not combine actual problems with simulation verification, and their practicability is not strong.

This paper will start with the power generation fault along the surface of a substation GIS basin insulator, analyze the cause of the fault, and establish a calculation model to simulate and analyze the surface field strength of the basin insulator, verify the cause of the fault, and conduct modeling and simulation of the model insulator to verify the correctness of the analysis. Put forward effective measures to avoid the recurrence of this type of problem in the expansion project.

2 Accident on-site inspection

At 13:15 on January 16, 2018, the relay protection staff of a power supply bureau handled the abnormal defect of 220kV GIS B set of bus differential protection current transformer in a 220kV substation. The work content was to replace the B set of 220kV bus coupler 210 switch A phase current transformer.The replacement of the capture card ends at 14:56, and the power is restored to check the working status of the capture card. At 16:25, the dispatch ordered the 220kV bus coupler 210 switch to switch from cold standby to operation.

At 18:08:08, turn on the 210 switch. At 18:08:26, the 220kV bus differential A and B sets of the protection of the substation acted, and the 210 switch was tripped.

After on-site inspection and equipment opening inspection, it was found that there was severe discharge at the top of the transition section between manufacturers A and B (plant A side), and there was no discharge trace on the other side of the basin insulator (plant B side), only on the conductor Scattered with white powder. On January 25, 2018, the factory staff conducted a physical inspection of the GIS of the fault section on the spot. Serious discharge marks were found on the surface of the ventilated basin insulator on the fault side, and a large amount of dust was scattered on this side, which is due to the effect of SF6 gas on the arc. The resulting material is shown in Figure 1.

Fig. 1 Vent basin insulator and conductor at fault side

The B and C three-phase conductors have serious discharge traces on the base roots, and the B and C traces are more obvious. There are some traces on the edge of the shell, and no discharge traces are found in other parts. As shown in Figures 2, 3, and 4.

Fig. 2 Phase A conductor base

Fig. 3 Phase B conductor base

Fig. 4 Phase C conductor base

Comparing the three-phase discharge situation, it can be seen that the interphase electric field distortion degree of the base is higher than the electric field of the conductor to the shell. No discharge traces were seen on the non-faulty side vented basin insulator and conductor fixing base.

3 Cause analysis

Preliminary analysis is based on the premise that the insulation margin of the GIS gas chamber design is relatively low, and due to the operating over voltage caused by the bus tie switch closing, the transition conductor structure of the wide and narrow barrel diameter and the voltage equalization base of the conductor root The phase-to-phase aggravated the distortion of the electric field, and then caused the surface discharge phenomenon on the surface of the failed basin insulator, which eventually led to the occurrence of the failure.

4 Modeling and simulation

4.1 Calculation principle and method

The finite element method is a discretized numerical method[10]. The principle is to divide the continuous physical structure into different areas, called units, and the subsequent numerical calculation and analysis will be carried out on these discrete units. In the electrostatic field, the potential is generally taken as the direct solution object. In an isotropic, linear, and uniform medium, the potential satisfies Poisson's equation or Laplace's equation:

$$\nabla^2\varphi = \frac{\rho}{\varepsilon} \text{ or } \nabla^2\varphi = 0 \tag{1}$$

The definite solution conditions are generally divided into four types:

Given the potential value on the boundary of the entire field, $u = f(P)$ is called the first type of boundary value problem.

Given the value of the electric potential method on the boundary of the entire field, $\frac{\partial u}{\partial n} = f(P)$ is called the second type of boundary value problem.

Given the linear combination of the potential on the boundary of the entire field and its normal guide number, $u(P) + \frac{\partial u}{\partial n} = f(P)$ is called the third type of boundary value problem.

In the mixed boundary value problem, the potential value is given on part of the boundary of the entire field, and the normal guide value of the potential is given in the remaining part. That is, $u|_{\Gamma_1} = f_1(P), \frac{\partial u}{\partial n}|_{\Gamma_2} = f_2(P)$, where Γ_1 and Γ_2 form the entire boundary of the field. Such problems are called mixed boundary value problems.

The calculation steps of the finite element method are as follows:

(1) Clarify the scope of the field and divide the field into finite units.

(2) Calculate the elements of the element's electric field energy coefficient matrix.

(3) Calculate the elements of the total electric field energy coefficient matrix.

(4) List the finite element equation [K][φ]=[B]-[P]

In the formula: [φ]——Internal node potential column vector;

[K]——n×n order coefficient matrix;

[B] ——Free item list vector;

[P] ——The second type of boundary value column vector.

(5) Solve the finite element equation and find the potential of each node.

(6) According to the potential of each node, the other quantities of the electric field can be obtained.

The finite element method can calculate and solve the electromagnetic field problem of the complex physical field. This project applies the large-scale finite element simulation calculation method to carry out the electric field check calculation of the 220kV substation equipment failures.

4.2 Boundary conditions for electric field calculation

In order to accurately calculate the field strength value of the faulty GIS equipment under the lightning impulse voltage, the electric field check of this type of GIS is realized. In the simulation calculation, the applied rated lightning impulse voltage amplitude and application method are consistent with the type test, that is, a voltage of 1050kV is applied in one phase, and the other two phases and the shell remain grounded, as shown in Figure 5.

The conductivity of the conductor is set to 38000000 siemens/m, the relative permittivity is 1, the relative permittivity of SF6 gas and basin insulator are 1.06 and 3.6, respectively, and the conductivity is 0.

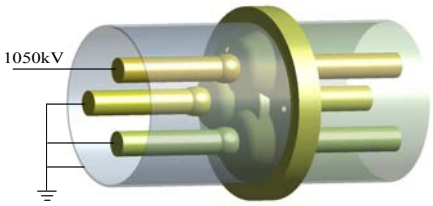

Fig. 5 Simulation calculation of voltage application mode

4.3 Simulation verification

The simulation software is Ansys. Apply 1050kV to phase A, and ground phase B/C. The overall distribution of the electric field in this case is shown in Figure 6. It can be seen that the electric field concentration area is the area between the A-phase conductor shield and the shell side and the convex basin insulator and the shell.

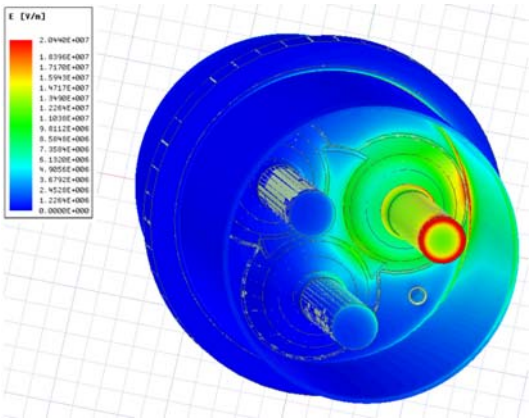

Fig. 6 Phase A is pressurized, phase B / C is grounded, the electric field is distributed as a whole

The distribution of the field strength on the conductor surface is shown in Figure 7. The maximum field strength is located on the side of the conductor shield close to the shell, the field strength value is m1=19.67kV/mm, and the field strength values at other positions of the conductor m2, m3, m4, and m5 are respectively 16.82kV/mm, 17.11kV/mm, 17.15kV/mm, 17.29kV/mm. The design reference value of the conductor surface field strength is recommended to be E1b=22.79kV/mm, and the conductor surface field strength has a certain margin.

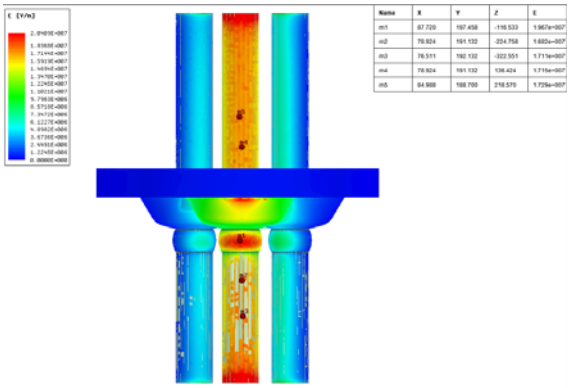

Fig. 7 Field strength distribution on conductor surface

The field strength distributions of the convex and concave surfaces of the basin insulator are shown in Figure 8 and Figure 9, respectively. The field strength values of the convex surface at positions m1, m2, m3, m4, m5, and m6 are 9.82kV/mm, 15.12kV/ mm, 17.87kV/mm, 37.47kV/mm, 10.71kV/mm, 8.998kV/mm. The field strength values of the concave surface at positions m1, m2, m3, m4, and m5 are 11.69kV/mm, 9.865kV/mm, 20.10kV/mm, 9.35kV/mm, 7.805kV/mm, respectively. The design reference value of the surface field strength of the insulator is Eτ=11.395kV/mm. The surface field strength values near m2 and m3 of the convex side of the basin insulator both exceed the design reference

value. The field strength value of the adjacent part of the basin insulator and the shell Much higher than other locations.

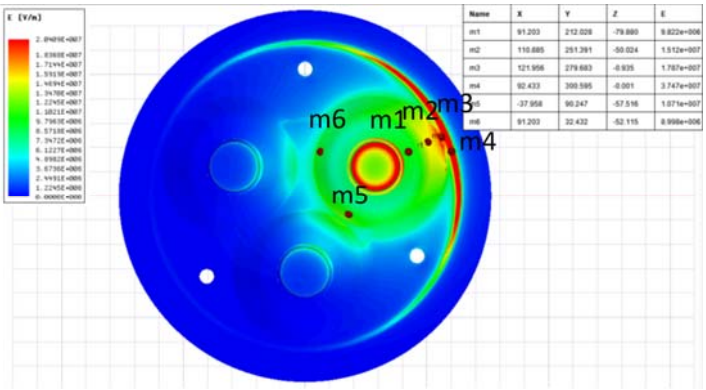

Fig. 8 Field strength distribution on convex surface of pot insulator

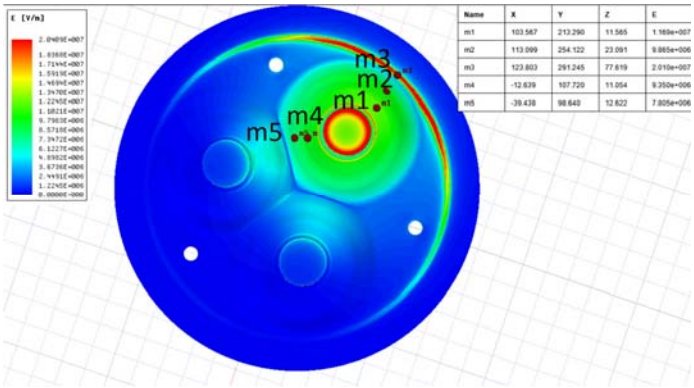

Fig. 9 Field strength distribution on concave surface of pot insulator

In the same way, apply 1050kV phase B, phase A/C to ground, and observe the field intensity distribution of phase B.Apply phase C 1050kV, phase A/B to ground, and observe the field intensity distribution of phase C.

Comprehensively considering the field strength distribution simulation results of the three phases A, B, and C, it is concluded that:

(1)There is a strong distorted electric field on the surface of the basin insulator;

(2)The electric field strength of the conductor surface is lower than the design reference value of the field strength, with a certain margin;

(3)The surface field strength of the convex surface of the basin insulator is higher than that of the concave surface;

(4)The surface field strength value of the convex area of the basin insulator is higher than the design reference value of the field strength;

(5)The field strength of the convex and concave surfaces of the basin insulator near the inner surface of the shell is much higher than that of other parts;

(6)The field strength value between the convex surface of the basin insulator B and C is higher than that of A and B, and A and C, which is more consistent with the surface discharge of the B and C basin insulators on site than in A.

The simulation results verified the analysis of the cause of the failure, and the overvoltage aggravated the distortion of the electric field on the surface of the basin insulator, and then the creeping discharge occurred.

5 Measures and suggestions

(1) In the time of GIS expansion, it is not allowed to adopt wide-narrow transitional GIS structure design.

(2) The insulation margin of basin-type insulators should be fully assessed.

(3) For the GIS interval designed for the wide and narrow transition structure of the grid stock, it is necessary to increase the partial discharge monitoring device, and periodically analyze the partial discharge test data, and deal with the power outage when necessary to prevent the expansion of defects.

6 Conclusion

Based on a 220kV GIS basin-type insulator along the surface discharge accident, through the analysis of site disintegration and historical operation and maintenance information, it is pointed out that insufficient insulation margin caused by unreasonable design is the main reason for the failure. Model insulators were modeled and simulated to verify the correctness of the analysis. The proposed measures provided a reference for the expansion of the GIS project.

References

1. Li Peng, Li Jinzhong, Cui Boyuan, et al. The latest technological development of UHV AC transmission and transformation equipment[J]. High Voltage Engineering, 2016, 42(04):1068-1078.
2. Qi Bo, Gao Chunjia, Xing Liangliang, et al. Surface charge distribution characteristics of GIS insulators under DC/AC voltage[J]. Proceedings of the CSEE, 2016(36):5990-6001.
3. Yang Wei, Zhu Taiyun, Tian Yu, et al. Transient electric field analysis of GIS basin insulators under lightning impulse voltage[J]. High Voltage Engineering, 2020(3):8.
4. Niu Bo, Tang Xin, Zhang Xinyi, et al. Research on Vibration Characteristics of Voltage Transformer in Gas Insulated Combined Electrical Apparatus[J]. High Voltage Apparatus, 2019, 55(11):5.
5. Li Chuanyang, Lin Chuanjie, Chen Geng, et al. A review on the charge behavior of the gas-solid interface of high voltage direct current basin insulators[J]. Proceedings of the CSEE, 2020, 40(6):10.
6. Xu Yang, Zhou Dianbo, Ding Dengwei, et al. Partial discharge detection of surface defects of GIS basin insulators[J]. High Voltage Apparatus, 2020, 56(5):6.
7. Zang Xu, Ma Hongzhong, Wu Jinli, et al. GIS discharge fault diagnosis based on improved approximate entropy of lumped empirical mode[J]. High Voltage Apparatus, 2020, 56(6):9.
8. He Baina, Kong Jie, Ning Jiaxing, et al. Electric field simulation analysis of basin insulator with bubble defect[J]. Insulating Materials, 2019, 52(5):7
9. Li Jinhui. Causes and precautions for flashover of basin insulators in GIS AC withstand voltage test[J]. Electrical Technology, 2018, v.19;No.227(09):133-135+141.
10. Wang Xucheng. Fundamental Principles and Numerical Methods of Finite Element Method [M]. Tsinghua University Press, 1997.